

Developmental plasticity and the origin of tetrapods

Emily M. Standen¹, Trina Y. Du² & Hans C. E. Larsson²

The origin of tetrapods from their fish antecedents, approximately 400 million years ago, was coupled with the origin of terrestrial locomotion and the evolution of supporting limbs. *Polypterus* is a member of the basal-most group of ray-finned fish (actinopterygians) and has many plesiomorphic morphologies that are comparable to elpistostegid fishes, which are stem tetrapods. *Polypterus* therefore serves as an extant analogue of stem tetrapods, allowing us to examine how developmental plasticity affects the ‘terrestrialization’ of fish. We measured the developmental plasticity of anatomical and biomechanical responses in *Polypterus* reared on land. Here we show the remarkable correspondence between the environmentally induced phenotypes of terrestrialized *Polypterus* and the ancient anatomical changes in stem tetrapods, and we provide insight into stem tetrapod behavioural evolution. Our results raise the possibility that environmentally induced developmental plasticity facilitated the origin of the terrestrial traits that led to tetrapods.

The evolution of terrestrial locomotion in vertebrates required the appearance of new behaviours and supporting appendicular structures^{1–8}. The skeletal changes included the origin of supporting limbs, the decoupling of the dermal pectoral girdle from the skull and the strengthening of the girdle ventrally for support⁹. The predicted behavioural changes at this transition include the planting of the pectoral fins closer to the midline of the body, thereby increasing the vertical component of the ground reaction force and raising the anterior body off the ground^{4,5,10}. How these evolutionary changes arose at the origin of tetrapods is still largely unclear, and the evolutionary processes surrounding these ancient events are not accessible because the transitional animals are extinct.

Environmentally induced phenotypes and their subsequent incorporation into heritable material may play an important role in macroevolution, including in the origin of novel traits^{11,12}. Phenotypic plasticity is the ability of an organism to react to the environment by changing its morphology, behaviour, physiology and biochemistry¹¹. Such responses are often beneficial for the survival and fitness of an organism and may facilitate success in novel environments^{13–15}. Phenotypically plastic traits can also eventually become heritable through genetic assimilation, which fixes a reduced range of phenotypic plasticity by decreasing a trait’s environmental sensitivity^{11,16,17}.

Major transitions that involved the modification and appearance of complex or novel traits may be accessible through the existing developmental pathways that allow plasticity in an ancestor. The ‘flexible stem’ model describes a process by which the fixed phenotypes of ecologically specialized lineages reflect the assimilation of alternative phenotypes by the ancestral lineage^{11,18–20}. For example, when marine sticklebacks were raised on alternative diets, developmental plasticity in the head shape and mouth shape paralleled the phenotypic divergence in the derived ecotypes¹⁹. Examining plasticity in an extant form may therefore shed light on the epigenetic processes in past evolutionary events^{11,12,19}.

This Article relates plasticity in an extant fish taxon to a major evolutionary transition: the origin of tetrapods. The plasticity of ancient fish might have provided the variation necessary to allow the evolution of the terrestrially functional fins that eventually evolved into limbs. Validating such a prediction is difficult as stem tetrapods are extinct. In these cases,

a sister taxon to the derived groups of interest can be used to estimate the ancestral plasticity¹².

In this study, we investigated developmental plasticity in *Polypterus*, the extant fish closest to the common ancestor of actinopterygians and sarcopterygians²¹. We chose *Polypterus* because it is one of the best models for examining the role of developmental plasticity during the evolution of stem tetrapods. *Polypterus* has an elongate body form, rhomboid scales, ventrolaterally positioned pectoral fins and functional lungs, all traits that are comparable to elpistostegid fishes. Moreover, this living fish is capable of surviving on land and can perform tetrapod-like terrestrial locomotion with its pectoral fins (E.M.S., T.Y.D., P. Laroche, B. Wilhelm and H.C.E.L., manuscript in preparation). Other terrestrially locomotory fish are derived teleosts that use a range of different gaits and have derived morphologies. Extant sarcopterygians (that is, lungfish (Dipnoi) and coelacanths (*Latimeria chalumnae*)) do not use their fins for terrestrial locomotion. By using an animal that already displays a walking behaviour, such as *Polypterus*, we can compare how obligatory walking influences gait and skeletal structure.

We raised control and treatment groups of *Polypterus* under aquatic and terrestrial conditions, respectively, to examine their behavioural and anatomical plasticity in response to a terrestrial habitat. By placing this predominantly aquatic animal in an obligatory terrestrial environment, we changed the forces experienced by the animal’s musculo-skeletal system. We predicted that the increased gravitational and frictional forces experienced by terrestrialized fish would cause changes in the ‘effectiveness’ of their locomotory behaviour when travelling over land, as well as changes in the shape of the skeletal structures used in locomotion. We also predicted that the plastic responses of the pectoral girdle of terrestrialized *Polypterus* would be similar to the directions of the anatomical changes seen in the stem tetrapod fossil record.

Swimming versus walking behaviour

During steady swimming, *Polypterus* oscillates its pectoral fins for propulsion, with little body and tail motion. *Polypterus* can also walk on land using a contralateral gait, by using its pectoral fins to raise its head and anterior trunk off the ground and by using its posterior body for forward

¹Biology Department, University of Ottawa, Gendron Hall, 30 Marie Curie Private, Ottawa, Ontario K1N 6N5, Canada. ²Redpath Museum, McGill University, 859 Sherbrooke Street West, Montreal, Quebec H3A 0C4, Canada.

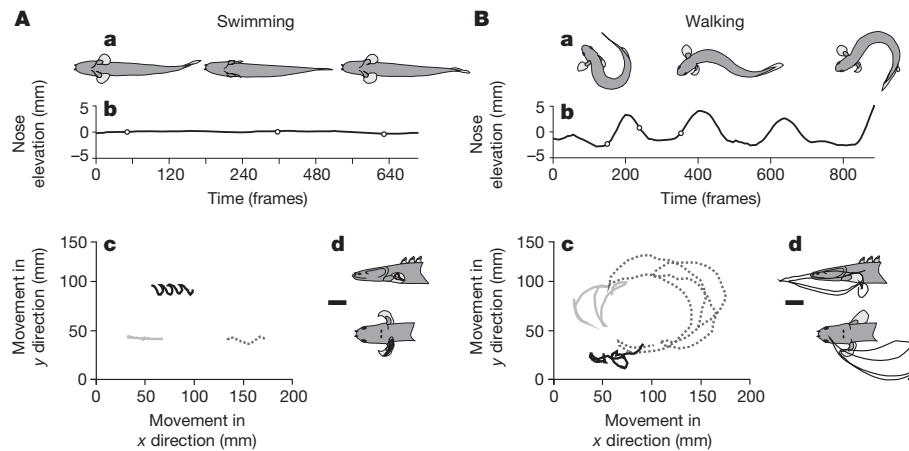


Figure 1 | Kinematic behaviour of swimming and walking *Polypterus*. **A**, Swimming in one exemplar fish. **B**, Walking in one exemplar fish. **a**, Maximum and minimum body curvature over one stroke cycle. **b**, Change in nose elevation over several stroke cycles (filmed at 250 frames s⁻¹). The circles correspond to the illustrations (from left to right) in **a**. **c**, Movement in the x–y plane (parallel to the ground) of the nose (solid grey line), tail (dotted grey line)

propulsion (Supplementary Video 1; E.M.S., T.Y.D., P. Laroche, B. Wilhelm and H.C.E.L., manuscript in preparation). We observed critical performance differences between swimming and walking (Fig. 1 and Extended Data Table 1). When *Polypterus* swam with a pectoral fin gait, it moved farther and faster per fin beat than when it walked. When walking, the fish moved their bodies and fins faster, and their nose, tail and fin oscillations were larger. Walking fish also had higher nose elevations, longer stroke durations and greater body curvatures. These performance differences suggest that walking is energetically more expensive than swimming²².

Biomechanical response to living on land

The treatment group of fish (which was raised on land) walked differently from the control group of fish (which was raised in water) (Extended Data Tables 1 and 2). The fish that were raised on land had their fins planted on the ground for less time and had shorter stride durations. Despite the faster stroke cycle of the treatment group fish, both treatment and control fish had comparable duty factors (approximately 0.65). Planted fins always slipped during the fin plant phase of the stroke, but the duration and distance of this potentially expensive fin ‘slip’ were shorter in the fish raised on land. The land-raised fish also had smaller pectoral fin excursions and elevations, planted their fins closer to the body midline, and had higher nose elevations and smaller tail oscillations. Reduction of unnecessary fin and tail motion and fine-tuning of fin placement to reduce body friction with the ground are required to minimize energy expenditure during walking, suggesting that the terrestrially-raised *Polypterus* has a more efficient gait.

The timing of critical kinematic variables is also important when determining performance. During walking, for both groups of fish, the fin was first planted near its most forward position, and the body was maximally curved, with the tail closest to the head. With the fin grounded, the tail pushed forwards, vaulting the anterior body and head over the planted fin. This positioning suggests that both fin and tail work together as the main thrust producers. The body curvature, tail amplitude, nose elevation and the start of the fin plant had similar timings in the stroke cycle for both groups of fish despite the differences in the environments in which the fish were raised (Fig. 2a, Extended Data Table 3 and Supplementary Video 1). These similarities indicate that walking with fins has basic kinematic requirements that are not necessarily improved with practise or competence. By contrast, the treatment group fish had a predictable timing for the majority of walking variables, whereas the control fish exhibited high degrees of variation. Importantly, the fin slide start occurred later during walking in the land-raised fish than in the water-raised fish. Additionally, the maximum forward (abduction) and

backward (adduction) fin position, the end of the fin plant, the end of the fin slide and the minimum distance from the fin to the body midline occurred at specific times within the stroke cycle in land-raised fish but were unpredictable in water-raised fish (Fig. 2 and Extended Data Table 3). These differences in timing between the control and treatment fish groups may indicate that the fish raised on land have a conditioned ‘training’ advantage.

During walking, in all fish, the maximum nose elevation and the beginning of the fin slide occurred half way through the head swing, when the nose crossed the forward path (Fig. 2b). The co-occurrence of these factors supports the hypothesis that the fin acts as a pole over which the head and anterior body are vaulted. Ground friction caused by the body and the amount of time the head and body are held off the ground must be limited and balanced to reduce the energy expenditure during walking. The treatment group fish had higher nose elevations and shorter

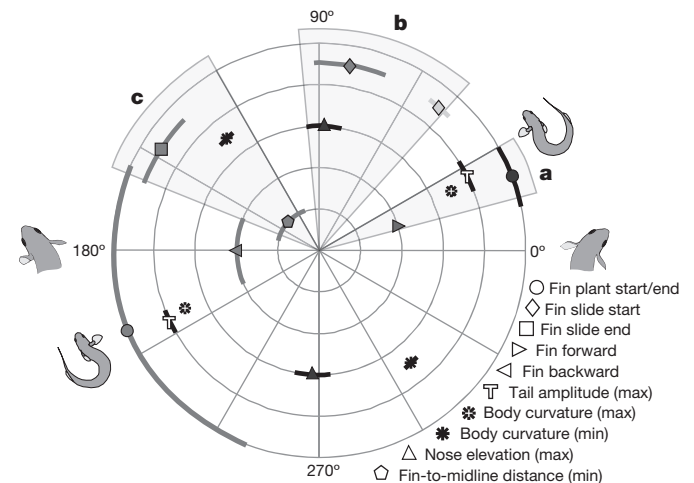


Figure 2 | Timing of kinematic variables for the left fin during walking in control and treatment group fish. One complete stroke cycle is represented by 360°. The stroke starts at 0° (head on the right). Mid-stroke occurs at 180° (head on the left). The stroke ends at 360° (0°). Data with significant directionality (Rayleigh’s test, $P < 0.05$) are plotted for the treatment group (dark grey, $n = 12$) and the control group (light grey, $n = 6$). Variables with similar timing between groups ($P > 0.05$) were binned and plotted as one (black). The symbols represent the mean timing (\pm angular variance, shown as a line) of the different kinematic variables. Some symbols occlude an extremely small angular variance. The areas highlighted in light grey (**a**, **b**, **c**) are key kinematic points in the stroke cycle. max, maximum; min, minimum.

stroke cycles, suggesting that the body ground friction and head elevation time were minimized. Additionally, the treatment group fish had less fin and body motion, less fin slip and less time between the start of the fin slide and the maximum head elevation, with the head and anterior body more effectively vaulting over the fin, possibly minimizing the energy loss due to slip. This difference in what seems to be a fundamentally important characteristic in walking over land hints that differences in control and/or 'effectiveness' during walking depend on an individual's training environment.

The treatment group fish also had a minimized distance between their planted fin and their body midline at the same time their fin stopped sliding (Fig. 2c). Bringing the fin closer to the midline generates more vertical ground reaction force through the fin, explaining the reduced fin slip. Control fish planted their fins farther from their body midline. These variables are critical for minimizing the effort required to move the body weight over land²³. By precisely controlling fin placement and fin slide timing, the treatment group fish may be streamlining the power that is required by the tail and the body to push the fish forwards by ensuring that the tail and body thrust occur when the body and head are lifted by the fin. Furthermore, the treatment group fish kept their fins stationed on the ground for the remainder of the step, allowing the fin to contribute to force production and control during the final phase of the step, and for the initiation of the next contralateral step. These behavioural differences are hypothesized to be 'learned' training advantages. Conversely, control fish had more variable fin slip timing, which lasted longer, as well as inconsistent timing patterns for the end of the fin plant, suggesting that they had not optimized their biomechanical performance.

The minimal differences in the kinematic variables between the treatment and control groups during swimming indicate that there was minimal 'loss' of swimming function associated with being raised in a terrestrial environment without the ability to 'practise' swimming after gill absorption (Extended Data Tables 1 and 4, Extended Data Fig. 1 and Methods).

Anatomical response to living on land

Like the biomechanical properties, the pectoral anatomy of land-raised *Polypterus* also exhibited phenotypic plasticity in response to terrestriation. The clavicle, cleithrum and supracleithrum of the fish pectoral girdle create a supporting brace that links the head and the body during locomotion and feeding (Fig. 3a). In most fish, including *Polypterus*, the paired clavicles are ventral, attaching to the anterior tip of the cleithrum medially and joining in symphysis at the midline, acting as a structural support for the neck and pectoral girdle²⁴. The cleithrum serves as an attachment point for muscles connecting to the skull anteriorly, to the trunk muscles posteriorly and to the pectoral fin muscles laterally²⁵. The supracleithrum articulates with the cleithrum and joins the pectoral girdle to the skull via the posttemporal bone.

The clavicle and cleithrum had significantly different shapes in the land-raised and water-raised groups (Fig. 3). The treatment group fish had narrower and more elongated clavicles, with more pointed processes that were 10.6% longer ($P \leq 0.046$). The clavicle cross-section was thinner in treatment group fish, in which the clavicle forms a cup that conforms to the cleithrum contact (Fig. 3c). In the land-raised fish, the cleithrum's horizontal arm also had a narrower lateral surface (Fig. 3b). Increased forces in the pectoral girdle from gravitational and postural changes may have induced a modelling response of the clavicle and cleithrum²⁶. Differences in bone shape may also reflect the need for increased fin mobility in terrestrial environments. When *Polypterus* walks, its fins must move through a larger range of motion than when it swims, forcing the operculum to bend out of the way to accommodate forward fin excursion. The posterior margin of the opercular cavity is displaced caudally by a reduction of the cleithrum's lateral postbranchial lamina. This change, along with the increased length and slenderness of the clavicle in treatment group fish, expands the opercular cavity between the fin and the operculum, providing more space for the pectoral fins to move.

Overall, the supracleithrum did not have a significantly different shape in water-raised and land-raised fish, but it was the only bone with an

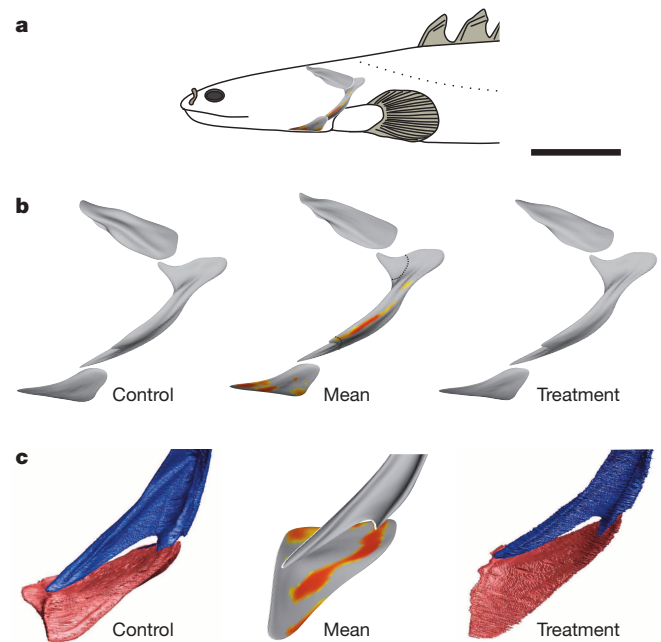


Figure 3 | Anatomical plasticity of *Polypterus* pectoral girdles. **a**, Location of the supracleithrum, cleithrum and clavicle in *Polypterus*. Scale bar, 1 cm. **b**, Left lateral views of the pectoral girdle with the mean clavicle (bottom), mean cleithrum (centre) and mean supracleithrum (top) dissociated for control (left) and treatment (right) group fish. A point-based multivariate analysis of covariance (MANCOVA) with correction for multiple comparisons (false discovery rate estimation) was used to determine the significant differences between the control ($n = 7$) and treatment ($n = 15$) *Polypterus* groups; significantly different regions are shown in colour (yellow, $P < 0.05$; red, $P < 0.01$). The mean illustration represents the average shape calculated from all individuals. **c**, Close-up anterolateral views of the mean clavicle (pink)–cleithrum (blue) contact in control (left) and treatment (right) group fish and the mean shape calculated from all individuals (centre).

allometric difference between the groups (Extended Data Table 5). The supracleithrum of the treatment group fish maintained the slenderness present at smaller bone sizes, with both the anterior process and posterior margin remaining narrow in the largest specimens and maintaining an underdeveloped midlateral ridge. The supracleithrum of control fish showed the opposite trend, developing robust anterior and posterior processes and midlateral ridges with increasing bone size. A size-related reduction in the supracleithrum's robustness may reflect a weakened connection to the posttemporal bone anteriorly and to the cleithrum posteriorly. This possibility suggests a weakened attachment between the pectoral girdle and the skull in land-raised fish. The size independence of the low midlateral ridge in the treatment group fish may also allow greater flexibility between the supracleithrum and the overlying operculum, further enlarging the opercular cavity and further freeing the pectoral girdle from the skull. Finally, comparison of bootstrap confidence intervals for shape variance showed that the land-reared fish had a higher shape disparity of the cleithrum and supracleithrum (Extended Data Fig. 2).

Plasticity and the origin of tetrapods

Terrestrialized *Polypterus* displayed less-variable walking behaviour, planted their pectoral fins closer to their body midlines, lifted their heads higher and had less fin slip, allowing more effective vaulting of the anterior body over the planted fin. These features are performance-enhancing traits during terrestrial locomotion¹⁰. We predict that similar behavioural changes were present in stem tetrapods. These locomotory changes in *Polypterus* probably affected the forces experienced by the skeleton, influencing skeletal growth and changing bone shape²⁷. The differences in bone morphology observed between terrestrialized and water-raised

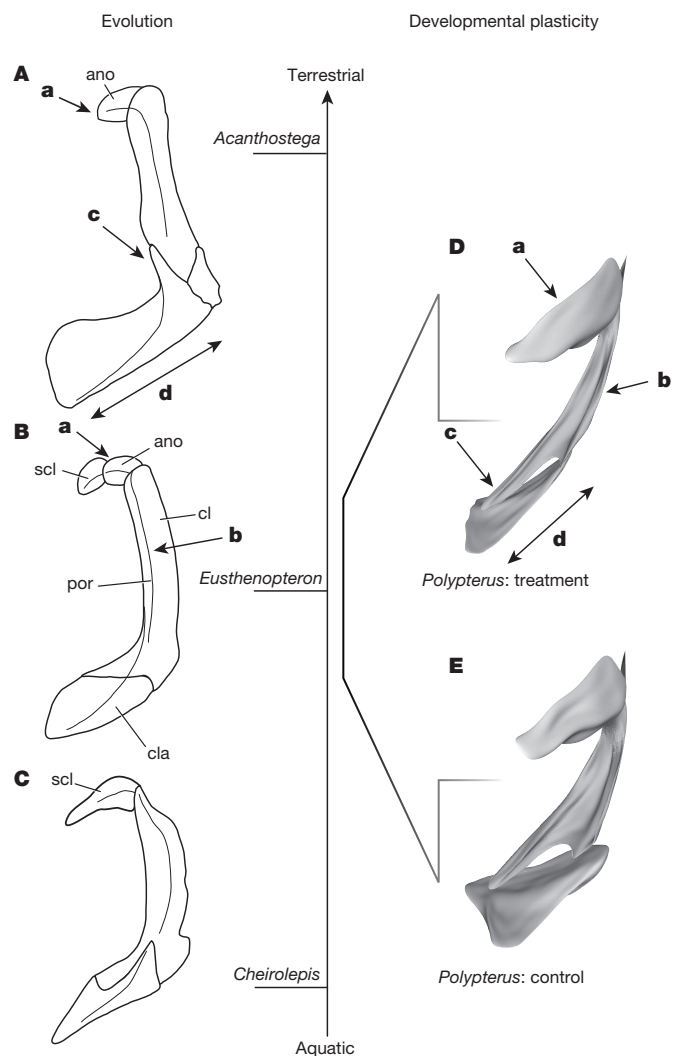


Figure 4 | Scenario for the contribution of developmental plasticity to large-scale evolutionary change in stem tetrapods. Left anterodorsolateral views of the pectoral girdle of selected stem tetrapods (A, B), an outgroup (C), and land-reared (D) and water-reared (E) *Polypterus*. The following are comparable developmentally plastic morphologies: reduction of the supracleithrum (a), reduction of the posterior opercular chamber edge (b), strengthened clavicle–cleithrum contact (c) and narrowing and elongation of the clavicle (d). ano, anocleithrum; cl, cleithrum; cla, clavicle; por, post opercular ridge (note the ridge in *Cheirolepis* is not distinct but is laterally positioned, as is shown); scl, supracleithrum.

Polypterus bear a remarkable resemblance to the evolutionary changes of stem tetrapod pectoral girdles during the Devonian period (Fig. 4). The skeletal changes seen in the treatment group fish revealed a marked reduction in the external boundaries of the opercular cavity bounded by the supracleithrum and cleithrum, which presumably facilitates greater flexibility between the pectoral girdle and the operculum, similar to what is observed in stem tetrapods such as *Eusthenopteron*²⁸. The elongation of the clavicles and the more tightly interlocking cleithrum–clavicle contact may strengthen the ventral brace through the clavicle, aiding in feeding, locomotion and body support in a terrestrial environment. Similar morphologies involving the medial bracing of the clavicles via an interclavicle are also thought to have stabilized the girdle in the earliest tetrapods, *Acanthostega* and *Ichthyostega*⁷. Finally, the dissociation of the pectoral girdle from the skull by reduction and loss of the supracleithrum and extrascapular bones allowed the evolution of a neck, an important feature for feeding on land⁹.

Novel or stressful environments, particularly those to which organisms have had no previous exposure or adaptations are catalysts for releasing variation^{29–31}. Evidence at a microevolutionary scale demonstrates that plasticity plays an important role in the appearance of complex traits^{18–20}. Our results show that exposure to a novel terrestrial environment can increase the phenotypic variation in the terrestrial locomotory behaviours and the pectoral girdle of *Polypterus*. We hypothesize that phenotypic plasticity, as a response to rapid and sustained environmental stresses, may also facilitate macroevolutionary change. Multi-generational experiments on terrestrialized *Polypterus* are required to determine the effect of developmental plasticity on the evolution of traits associated with effective terrestrial locomotion.

Developmental plasticity can be integrated into the study of major evolutionary transitions. The rapid, developmentally plastic response of the skeleton and behaviour of *Polypterus* to a terrestrial environment, and the similarity of this response to skeletal evolution in stem tetrapods, is consistent with plasticity contributing to large-scale evolutionary change. Similar developmental plasticity in Devonian sarcopterygian fish in response to terrestrial environments may have facilitated the evolution of terrestrial traits during the rise of tetrapods.

Online Content Methods, along with any additional Extended Data display items and Source Data, are available in the online version of the paper; references unique to these sections appear only in the online paper.

Received 26 March; accepted 24 July 2014.

Published online 27 August; corrected online 3 September 2014 (see full-text HTML version for details).

- Niedzwiedzki, G., Szrek, P., Narkiewicz, K., Narkiewicz, M. & Ahlberg, P. E. Tetrapod trackways from the early Middle Devonian period of Poland. *Nature* **463**, 43–48 (2010).
- Clack, J. A. The fin to limb transition: new data, interpretations, and hypotheses from paleontology and developmental biology. *Annu. Rev. Earth Planet. Sci.* **37**, 163–179 (2009).
- Callier, V., Clack, J. A. & Ahlberg, P. E. Contrasting developmental trajectories in the earliest known tetrapod forelimbs. *Science* **324**, 364–367 (2009).
- Shubin, N. H., Daeschler, E. B. & Jenkins, F. A. J. The pectoral fin of *Tiktaalik roseae* and the origin of the tetrapod limb. *Nature* **440**, 764–771 (2006).
- Pierce, S. E., Clack, J. A. & Hutchinson, J. R. Three-dimensional limb joint mobility in the early tetrapod *Ichthyostega*. *Nature* **486**, 523–527 (2012).
- Ahlberg, P. E. & Clack, J. A. Palaeontology: a firm step from water to land. *Nature* **440**, 747–749 (2006).
- Clack, J. A. *Gaining Ground* 2nd edn (Indiana Univ. Press, 2012).
- Coates, M. I. *Acanthostega gunnari Jarvik*: postcranial anatomy, basal tetrapod interrelationships and patterns of skeletal evolution. *Trans. R. Soc. Edinb. Earth Sci.* **87**, 363–421 (1996).
- Coates, M. I., Ruta, M. & Friedman, M. Ever since Owen: changing perspectives on the early evolution of tetrapods. *Annu. Rev. Ecol. Evol. Syst.* **39**, 571–592 (2008).
- Blob, R. W. & Biewener, A. A. Mechanics of limb bone loading during terrestrial locomotion in the green iguana (*Iguana iguana*) and American alligator (*Alligator mississippiensis*). *J. Exp. Biol.* **204**, 1099–1122 (2001).
- West-Eberhard, M. J. *Developmental Plasticity and Evolution* (Oxford Univ. Press, 2003).
- Moczek, A. P. et al. The role of developmental plasticity in evolutionary innovation. *Proc. R. Soc. B* **278**, 2705–2713 (2011).
- Ghalambor, C. K., McKay, J. K., Carroll, S. P. & Reznick, D. N. Adaptive versus non-adaptive phenotypic plasticity and the potential for contemporary adaptation in new environments. *Funct. Ecol.* **21**, 394–407 (2007).
- Price, T. D., Qvarnstrom, A. & Irwin, D. E. The role of phenotypic plasticity in driving genetic evolution. *Proc. R. Soc. Lond. B* **270**, 1433–1440 (2003).
- Yeh, P. J. & Price, T. D. Adaptive phenotypic plasticity and the successful colonization of a novel environment. *Am. Nat.* **164**, 531–542 (2004).
- Crispo, E. The Baldwin effect and genetic assimilation: revisiting two mechanisms of evolutionary change mediated by phenotypic plasticity. *Evolution* **61**, 2469–2479 (2007).
- Waddington, C. H. Genetic assimilation of an acquired character. *Evolution* **7**, 118–126 (1953).
- Gomez-Mestre, I. & Buchholz, D. R. Developmental plasticity mirrors differences among taxa in spadefoot toads linking plasticity and diversity. *Proc. Natl Acad. Sci. USA* **103**, 19021–19026 (2006).
- Wund, M. A., Baker, J. A., Clancy, B., Golub, J. L. & Foster, S. A. A test of the “flexible stem” model of evolution: ancestral plasticity, genetic accommodation, and morphological divergence in the threespine stickleback radiation. *Am. Nat.* **172**, 449–462 (2008).
- Rajakumar, R. et al. Ancestral developmental potential facilitates parallel evolution in ants. *Science* **335**, 79–82 (2012).
- Inoue, J. G., Miya, M., Tsukamoto, K. & Nishida, M. Basal actinopterygian relationships: a mitogenomic perspective on the phylogeny of the “ancient fish”. *Mol. Phylogenet. Evol.* **26**, 110–120 (2003).

22. Tucker, V. A. The energetic cost of moving about: walking and running are extremely inefficient forms of locomotion. Much greater efficiency is achieved by birds, fish—and bicyclists. *Am. Sci.* **63**, 413–419 (1975).
23. Kawano, S. M. & Blob, R. W. Propulsive forces of mudskipper fins and salamander limbs during terrestrial locomotion: Implications for the invasion of land. *Integr. Comp. Biol.* **53**, 283–294 (2013).
24. Gosline, W. A. The structure and function of the dermal pectoral girdle in bony fishes with particular reference to ostariophysines. *J. Zool.* **183**, 329–338 (1977).
25. Winterbottom, R. A descriptive synonymy of the striated muscles of the teleostei. *Proc. Acad. Nat. Sci. Philadelphia* **125**, 225–317 (1973).
26. Biewener, A. A. Scaling body support in mammals: limb posture and muscle mechanics. *Science* **245**, 45–48 (1989).
27. Frost, H. M. On our age-related bone loss: insights from a new paradigm. *J. Bone Miner. Res.* **12**, 1539–1546 (1997).
28. Andrews, S. M. & Westoll, T. S. The postcranial skeleton of *Eusthenopteron foerii* Whiteaves. *Trans. R. Soc. Edinb.* **68**, 207–329 (1970).
29. Badyaev, A. V. Stress-induced variation in evolution: from behavioural plasticity to genetic assimilation. *Proc. R. Soc. B* **272**, 877–886 (2005).
30. Suzuki, Y. & Nijhout, H. F. Evolution of a polyphenism by genetic accommodation. *Science* **311**, 650–652 (2006).
31. Lerouzcic, A. & Carlborg, O. Evolutionary potential of hidden genetic variation. *Trends Ecol. Evol.* **23**, 33–37 (2008).

Supplementary Information is available in the online version of the paper.

Acknowledgements We thank F. A. Jenkins Jr and C. R. Marshall for encouragement and discussions with E.M.S. during the initial phases of this project. We also thank E. Abouheif for discussions and editing of the manuscript. We thank J. Dawson for the loan of camera equipment, S. Bertram for access to laboratory space while running the experiment and B. Bongfeldt for animal care and preliminary data analysis. We are grateful for the Tomlinson Post-doctoral Fellowship (E.M.S.), for grants from the National Sciences and Engineering Research Council of Canada (PDF to E.M.S., CGS-M to T.Y.D. and Discovery Grant #261796-2011 to H.C.E.L.), for the Robert G. Goelet Research Award (E.M.S.) and to Canada Research Chairs (H.C.E.L.).

Author Contributions E.M.S. conceived, designed and conducted the experiments and biomechanical analyses. T.Y.D. scanned, segmented and analysed the micro-computed tomography images. H.C.E.L. provided palaeontological and evolutionary expertise that shaped the project. E.M.S., T.Y.D. and H.C.E.L. wrote the manuscript.

Author Information Reprints and permissions information is available at www.nature.com/reprints. The authors declare no competing financial interests. Readers are welcome to comment on the online version of the paper. Correspondence and requests for materials should be addressed to E.M.S. (estanden@uottawa.ca) or H.C.E.L. (hans.ce.larsson@mcgill.ca).

METHODS

Experimental protocol. Juvenile *Polypterus senegalus* were divided into two groups and raised in different environments for 8 months. One group was raised in an aquatic environment (control), and the other was raised in a terrestrial environment (treatment). Quantification of the anatomical and biomechanical changes was carried out, and the values were compared between groups to assess the effect of environment on developmental plasticity. All experiments were conducted under Carleton University animal care protocol B09-28 and McGill University animal care protocol #6000.

Rearing habitats. All fish were kept in a 300-gallon recirculating aquarium system that provided the control and treatment groups with identical water quality conditions over time. The water was kept at 78 ± 2 °F and cleaned with an active bio-filter. Fish were fed a high protein diet, and both groups received the same amount of food daily. Control animals were kept in an aquatic environment with a water depth maintained at 210 mm. Treatment group animals were raised in a terrestrial environment (water depth 3 mm). Water misters provided a continual mist in the terrestrial environment to prevent desiccation. The terrestrial environments also had a mesh flooring scattered with pebbles to stimulate climbing and navigating non-uniform surfaces and to provide habitat complexity, reducing negative fish interactions. The terrestrial and aquatic environments had plants to provide habitat complexity.

Fish. Animals were acquired through the pet trade (Mirdo Importations). Because this study addresses how environment influences growth, animals were acquired as young as possible, but after gill absorption to ensure survival during shipping. All animals possessed juvenile markings on arrival, suggesting that they were less than 70 days old³². Reliable non-invasive sex determination of juvenile *Polypterus* is not possible; as a result, animals were kept and studied in unmarked mixed-sex groups. Animal growth was monitored by assessing the length and weight of fish upon entry to the environments and after 8 months of growth within the environments. The length and weight of fish were measured and compared as pooled groups because individual fish were too small to be identified individually over time. All measurements were made by photographing individuals and then calibrating and digitizing the images.

Before arrival, all fish had been raised in fully aquatic environments ($n = 149$). Although most fish still exhibited strong juvenile markings upon arrival, any fish that had fainter stripes were assumed to be older and were left in the aquatic control group, as they had been in an aquatic environment from their beginning. The remaining fish were divided into the aquatic environment (control, $n = 38$) and the terrestrial environment (treatment, $n = 111$) groups. Because fish were distributed in this fashion, size differences existed between the groups (Extended Data Table 6). This initial size difference was taken into consideration when determining the changes in fish size due to treatment environments, by bootstrapping the length and weight data 10,000 times at the start and end of the trials to generate means for comparison before and after treatment (Extended Data Fig. 3). Fish numbers were chosen and distributed in this way because of limitations in habitat area within the experimental set-up and in anticipation of higher mortality in terrestrial environments.

Camera filming and calibration for biomechanical analysis. All behavioural sequences were filmed at 250 frames s^{-1} using two synchronized Redlake Cameras (IDT Vision). A calibration device with known points was used to image the field of view for each camera. A direct linear transformation (DLT) algorithm³³ implemented in MATLAB using a DLT data viewer³⁴ used the above calibration images to calculate and quantify the volume of each field of view. From this, the three-dimensional location of any point within the field of view could be calculated. Video images were digitized manually using the DLT data viewer³⁴. Digitization was conducted without knowledge of the environment in which the filmed fish had been raised, to reduce digitizing bias.

Swimming behaviour. *P. senegalus* (control, $n = 10$; treatment, $n = 20$) was filmed swimming freely through a still water aquarium (1.5 feet wide \times 6 feet long \times 1 foot deep) to assess the kinematic performance of body and fin motion during steady swimming. The filming area (~ 20 cm \times 14 cm) was located in the centre of the aquarium to eliminate behavioural effects due to tank walls. Sequences in which fish swam steadily, demonstrating a minimum of three consecutive fin beats, were selected for analysis. Fish behaviour was very consistent: fish were randomly chosen from their rearing tanks, and each chosen fish was given one attempt to swim through the aquarium. All but one animal provided usable sequences. A subset of these sequences (control, $n = 6$; treatment, $n = 12$) was randomly chosen to be used in the analysis to maintain an equal sample size with the walking behaviour sample size. Sample size was chosen based on the estimated effect size calculated from the expected differences between the treatment and control groups. Cameras were situated below and beside the tank to provide clear views of the left pectoral fin during swimming.

Walking behaviour. *P. senegalus* (control, $n = 10$; treatment, $n = 20$) was filmed walking freely across a rough plastic surface (30 cm \times 30 cm) to assess the kinematic performance of body and fin motions during terrestrial locomotion. The filming area (~ 22 cm \times 20 cm) was located in the centre of the walking surface. Sequences in which fish walked steadily, demonstrating a minimum of three consecutive fin beats,

were selected for analysis (control, $n = 6$; treatment, $n = 12$). Fish were randomly removed from their rearing tanks and, to avoid exhaustion artefacts, each fish was only walked once and then returned to a holding tank until the experiment was completed. Cameras were situated above the walking platform, with one directly above the surface and one at an angle, to provide clear views of at least one pectoral fin during walking.

Biomechanical variables of interest. Owing to variation in kinematic performance between swimming and walking, the fin beat cycle was defined by different methods. During swimming, the start of the fin beat cycle corresponded to the fin being against the body of the fish. The mid-cycle corresponded to fin maximal abduction. The end of the cycle corresponded to the starting point of the next cycle. During walking, the starting point of the cycle corresponded to the maximum amplitude of the nose to the right. The mid-cycle was marked by the maximum displacement of the nose to the left. The end of the cycle corresponded to the start of the next fin beat. Overall locomotory performance was assessed by the distance travelled per fin beat, the fish velocity per fin beat and the overall fish path curvature. Both the magnitude and the timing of the kinematic variables were used to compare swimming and walking, as well as to compare the control and treatment groups.

Body kinematics. Body amplitude was calculated using the mediolateral motion of the tip of the nose and tail during swimming. A metric of overall body curvature was calculated as the distance between the nose and the tail divided by the fish length. Nose elevation was also measured as the relative change in the elevation of the tip of the nose over time. The maximum nose and tail velocities were also calculated. All variables were standardized by dividing by body length.

Fin kinematics. Fin elevation and fin motion in the x - y plane were calculated, as well as the overall fin velocity. Stroke duration was also calculated as the time it took for a fin to complete a full fin beat cycle. For walking fish, the fin plant duration and the fin slide duration were divided by the stroke duration to calculate the duty factor (the percentage of the fin cycle for which the fin is in contact with the ground) and the slip factor (the percentage of the fin cycle for which the fin is sliding along the ground). The distance that the fin slid over the ground during the fin plant (fin slide distance) was calculated as the straight line distance between the tip of the fin at the slide start and the slide end. The minimum distance between the planted fin and the body midline was calculated as the length of the normal vector from the fin tip to the line that is formed between the fish nose and the base of the first dorsal fin ray. All fin variables were standardized by dividing by fin length.

Timing. The timing of all kinematic variables was calculated in radians (Extended Data Tables 3 and 4). The fin cycle start (0 rad), mid-cycle (π rad) and end (2π rad) anchored each fin beat and allowed the variables to be plotted and to be compared between fin cycles.

Statistics. Statistical analysis was divided into two sections: timing and magnitude. For each variable, a maximum performance value was taken for each fish. Cycle timing (polar coordinates) was analysed using standard circular data analysis. Data were tested for von Mises distribution and equal variation (Kuiper test). Mean timing angles and 95% confidence intervals were calculated according to ref. 35, with angular variance calculated according to refs 36 and 37. Rayleigh's test for circular uniformity was conducted to determine whether the variables occurred at predictable times in the oscillation cycle. If the variables proved to have directionality based on Rayleigh's test, a two-sample testing of the mean timing angles was performed using an F statistic according to ref. 37. The timing of all variables was tested between the treatment group and the control group. The velocity, curvature and nose elevation data measurements during swimming and walking were treated as diametrically bimodal distributions, as they peaked twice in a single fin beat. The magnitudes of all kinematic variables were calculated using standard statistical procedures to calculate the mean and s.e.m.. The Mann-Whitney U -test was used to compare the means. The body and fin size of the fish were bootstrapped to achieve normal distributions and then compared between treatments and over time (Extended Data Table 6 and Extended Data Fig. 3). The significance levels for all tests were based on initial P values of < 0.05 . Permutation tests were used to generate a null distribution of test statistics against which the observed statistic was compared. Effect sizes were calculated using pooled standard deviations. All linear statistical tests were completed using JMP v8.0 (SAS Institute), MATLAB vR2006a and the R statistical environment. Circular statistical tests were conducted using a custom-made program within MATLAB. Measurements noted in the text are expressed as mean \pm s.e.m..

Spherical harmonics analysis (SPHARM). Micro-computed tomography (micro-CT)-derived three-dimensional volumes of fish pectoral skeletons were imaged and compared using SPHARM³⁸. SPHARM is the three-dimensional extension of two-dimensional elliptical Fourier analysis, a morphometric technique commonly used to describe closed outlines³⁹.

Three-dimensional surface generation. Fish from the treatment and control groups were randomly chosen and sacrificed, fixed in 4% paraformaldehyde then preserved in 70% ethanol. Specimens were scanned using a SkyScan 1172 micro-CT scanner. Owing to the sample dimension constraints of the scanner, only the portion anterior

to the distal extent of the pectoral fins was scanned. To prevent desiccation of the samples during scanning, the samples were wrapped in a thin layer of Parafilm, then wrapped with tissue paper to prevent movement inside the sample holder. The top half of a 15-ml centrifuge tube was used as a sample holder. All samples were scanned under identical scanning parameters. Cross-sectional images were reconstructed from the raw tomography projection images using NRecon reconstruction software (SkyScan). Pectoral girdle elements were segmented manually in Avizo 7 (FEI Visualization Sciences Group) and exported as binary volumes for analysis. Seven control fish and 15 treatment fish were randomly selected, preserved and scanned for this analysis. The sample size was determined by scanning and segmentation duration; the maximum number of samples was scanned given the resources available. Segmentation of all specimens was performed by the same person, and no blinding was done.

Surface processing and SPHARM expansion. Binary data were processed by removing holes, isotropic resampling and smoothing. The resultant closed three-dimensional volumes were then converted into surface meshes. Bijective mapping of the surface points onto a unit sphere generated a spherical parameterization that was expanded as a Fourier series. The resultant Fourier functions were then used to compute SPHARM coefficients up to 15 degrees. Point distribution models (PDMs) with homogeneous sampling of the object surfaces were then generated from the coefficients by uniform sampling of the spherical parameterization with an icosahedron subdivision of factor 10.

Alignment. An initial alignment rotated object surface parameterizations based on the major axes of their first order ellipsoids and ellipsoid origins. The preceding steps were performed using SPHARM-PDM⁴⁰ via the command line. After this initial alignment, object surfaces were imported into MATLAB and realigned with SPHARM-MAT³⁹ using a quaternion-based algorithm, which minimizes the least-squares distance between corresponding surface points. Owing to difficulties in achieving an acceptable initial alignment using the first order ellipsoids, the cleithral surfaces were first aligned using SPHARM-MAT. The aligned surfaces were then reconverted into binary volumes and passed through SPHARM-PDM as raw data. New spherical harmonic surface models and coefficients were then generated from these pre-aligned volumes and were not aligned again. This realignment process also produced size-normalized surface meshes. Scaling of the coefficients was performed in R, and the scaling factor was the inverse of the semi-major axis length of the first order ellipsoid.

Allometric analysis. Body growth, standardized to body length, was reduced in fish raised on land (Extended Data Table 6 and Extended Data Fig. 3), probably because of increased stress under terrestrial conditions. The effect of size on shape was evaluated in R, using a reduced number of SPHARM coefficients as variables. Ninety-nine coefficients were retained for the clavicle, 75 for the cleithrum, and 97 for the supraclavicle, accounting for at least 99% of the total coefficient variation in each element. To further reduce the number of response variables, a principal components analysis (PCA) was performed on the remaining coefficients, and the first four principal components axes were retained for analysis.

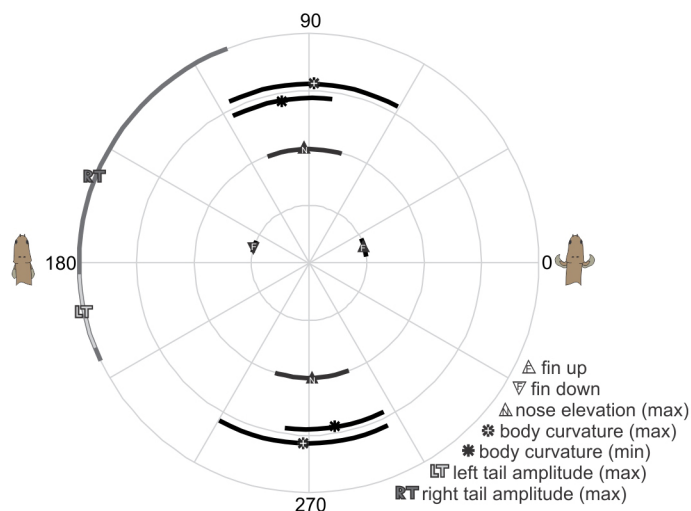
To test for the presence of allometry, shape variables (principal components scores) were fit to an analysis of covariance (ANCOVA) model with size as a continuous variable and rearing environment as a categorical variable. The significance of the terms was tested with an analysis of variance (ANOVA). To test whether the regression coefficients differed between treatment groups, a model including an interaction term between size and treatment was compared to a simply additive model using an ANOVA. Permutation tests were used to generate a null distribution of F statistics against which the observed F was compared.

The relative contribution of size to bone shape was calculated by performing a multivariate linear regression with size as the independent variable and harmonic coefficients as the dependent variable. The proportion of shape variance explained by size was then calculated by dividing the sum of the variances in fitted values by the sum of the diagonal of the variance-covariance matrix of the original coefficients. Allometric shape changes were visualized by comparing the shapes corresponding to the fitted shape variables at the minimum and maximum sizes. These coefficients from the hypothetical maximum and minimum shapes were imported into SPHARM-MAT, where their corresponding surface meshes were generated. When significant differences in regression coefficients were found between treatment groups, a separate regression and the corresponding maximum and minimum shapes were computed for each group.

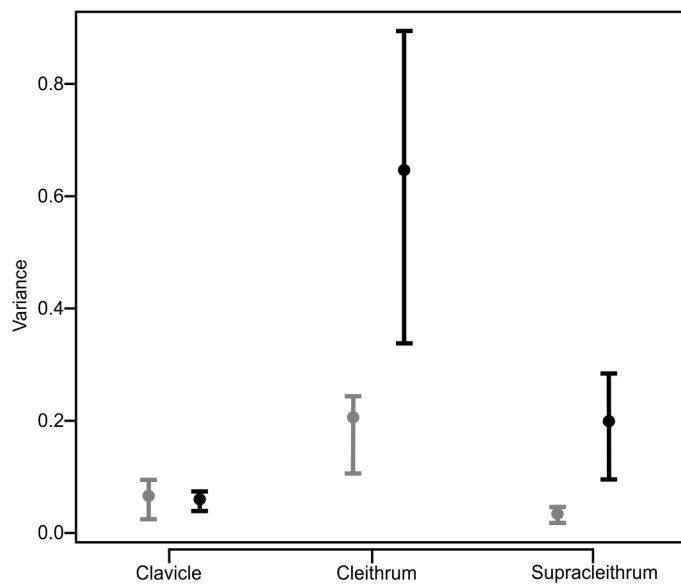
Point analysis. Local shape differences based on PDMs were also examined using ShapeAnalysisMANCOVA, an add-on program to SPHARM-PDM⁴¹. This method takes the surfaces produced by SPHARM-PDM and SPHARM-MAT, fits the coordinate data for the surface points to a general linear model including size as an independent variable, performs MANCOVAs on the displacement vectors between the observed surfaces and the overall mean shape and then calculates the Hotellings T^2 statistic. P values were computed using a non-parametric correction, which can be applied when the assumptions of a parametric approach are not met⁴¹. Ten thousand permutations were used at a 0.05 significance level. Multiple comparison errors were corrected using false discovery rate estimation with a 5% threshold.

Equal variance. Bootstrapped confidence intervals (95%) were used to test for homogeneity of shape variances between the control and treatment groups. The variance was calculated for each group by summing the squared principal components scores for the first four components then dividing by the number of specimens in the group. Permutation tests were used to generate a null distribution of differences in variance against which the observed difference was compared.

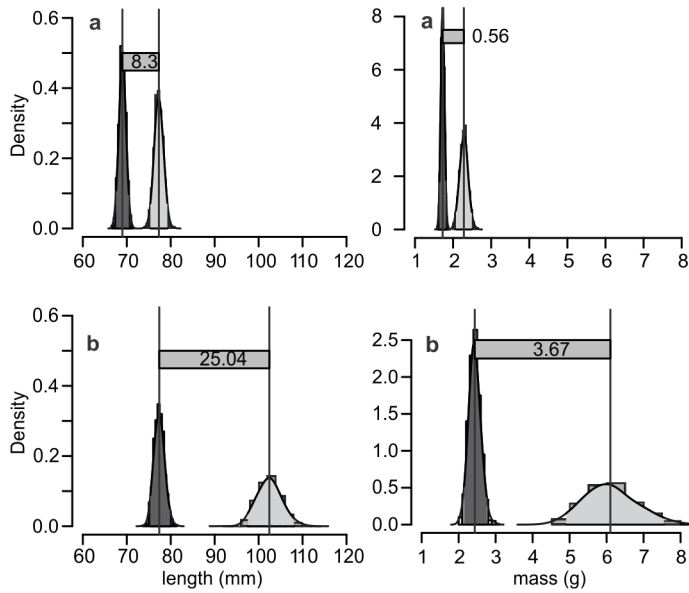
32. Bartsch, P., Gemballa, S. & Piotrowski, T. The embryonic and larval development of *Polypterus senegalus* Cuvier, 1829: its staging with reference to external and skeletal features, behaviour and locomotory habits. *Acta Zool.* **78**, 309–328 (1997).
33. Reinschmidt, C. & van den Bogert, T. KineMat: a MATLAB toolbox for three-dimensional kinematic analyses. <http://isbweb.org/software/movanal/kinemat/> (Human Performance Laboratory, Univ. Calgary, 1997).
34. Hedrick, T. L. Software techniques for two- and three-dimensional kinematic measurements of biological and biomimetic systems. *Bioinspir. Biomim.* **3**, 034001 (2008).
35. Zar, J. H. *Biostatistical Analysis*. 4th edn (Prentice Hall, 1999).
36. Batschelet, E. *Statistical Methods for the Analysis of Problems in Animal Orientation and Certain Biological Rhythms* (American Institute of Biological Sciences, 1965).
37. Batschelet, E. *Circular Statistics in Biology* (Academic, 1981).
38. Brechbühler, C. H., Gerig, G. & Kübler, O. Parametrization of closed surfaces for 3-D shape description. *Comput. Vis. Image Underst.* **61**, 154–170 (1995).
39. Shen, L., Farid, H. & McPeck, M. A. Modeling three-dimensional morphological structures using spherical harmonics. *Evolution* **63**, 1003–1016 (2009).
40. Styner, M. *et al.* Framework for the statistical shape analysis of brain structures using SPHARM-PDM. *Insight J.* <http://www.insight-journal.org/browse/publication/101> (11 July 2006).
41. Paniagua, B., Styner, M., Macenko, M., Pantazis, D. & Niethammer, M. Local shape analysis using MANCOVA. *Insight J.* <http://www.insight-journal.org/browse/publication/694> (10 September 2009).



Extended Data Figure 1 | Timing of kinematic variables for the left fin during swimming in control and treatment group fish. The polar plot represents a complete stroke cycle, starting at 0° with the fin fully adducted. At mid-stroke (180°), the fin is fully abducted, and then it adducts again (360°/0°). The data are plotted for the treatment group (dark grey, $n = 12$) and the control group (light grey, $n = 6$). Only data with significant directionality are plotted (Rayleigh's test, $P < 0.05$). If the groups did not differ significantly in the timing of a given variable, they were binned and plotted together (black). The symbols represent the mean timing (\pm angular variance) of different kinematic variables.



Extended Data Figure 2 | Variance in bone shape in control and treatment group fish. Bone-shape variances between the control group (light grey, $n = 7$) and the treatment group (dark grey, $n = 15$). Dots indicate observed variance; error bars indicate bootstrapped 95% confidence intervals.



Extended Data Figure 3 | Body length and mass in control and treatment group fish. Bootstrapped differences in mean body length and mass between water-raised and land-raised fish at the start (a) and end (b) of the experiment. At the start of the experiment, land-raised fish were smaller than water-raised fish (Extended Data Table 6). Similar size relationships existed between the control (light grey) and treatment (dark grey) groups at the end of the experiment, but the differences were much greater (Extended Data Table 6). Length and weight data at the start (control, $n = 38$; treatment, $n = 111$) and the end (control, $n = 30$; treatment, $n = 69$) of the experiment were bootstrapped 10,000 times, and means were generated from each bootstrap. These values were used to test how the mean difference between the groups changed from the start to the end of the experiment. In all cases, the differences between the control and treatment groups increased over time.

Extended Data Table 1 | Magnitudes of kinematic variables during walking and swimming

Variable*	Group	Walk mean ± s.e.m.	Swim mean ± s.e.m.	$P_{U(U-stat, df)}$, P_{Perm}^{\dagger}	Effect Size (P_{Power})
Distance / fin beat (BL)	Control	0.096±0.011	0.108±0.007	0.2402 _(10,10) , 0.0779	-1.1326 _(0,4261)
	Treatment	0.087±0.007	0.110±0.011	0.03872 _(36,22) , 0.0090	-1.0772 _(0,7130)
	$P_{U(U-stat, df)}$, P_{Perm} Effect Size (P_{Power})	0.4936 _(28,16) , 0.1938	0.9636 _(35,16) , 0.4965		0.0872 _(0,0531)
Velocity / fin beat (BL/sec)	Control	0.060±0.011	0.0683±0.005	0.2403 _(10,10) , 0.1009	-0.8070 _(0,2444)
	Treatment	0.038±0.004	0.0545±0.0042	0.0011 _(18,22) , 0	-1.5540 _(0,9531)
	$P_{U(U-stat, df)}$, P_{Perm} Effect Size (P_{Power})	0.1246 _(19,16) , 0.0450	0.102 _(18,16) , 0.035		-0.8987 _(0,3936) -1.0598 _(0,5127)
Path curvature‡ (k=1/radius, mm)	Control	0.035±0.015	0.022±0.005	0.6991 _(21,10) , 0.3087	0.6169 _(0,1624)
	Treatment	0.084±0.018	0.039±0.009	0.0007 _(128,22) , 0	1.3502 _(0,8849)
	$P_{U(U-stat, df)}$, P_{Perm} Effect Size (P_{Power})	0.0529 _(57,16) , 0.0230	0.1025 _(54,16) , 0.0400		1.04931 _(0,5049) -0.8414 _(0,3530)
Body curvature‡ (BL distance nose to tail)	Control	0.549±0.059	0.962±0.013	0.0022 _(36,10) , 0	-4.2100 _(0,1000)
	Treatment	0.547±0.035	0.960±0.007	0 _(144,22) , 0	-4.0503 _(1,0000)
	$P_{U(U-stat, df)}$, P_{Perm} Effect Size (P_{Power})	0.9636 _(35,16) , 0.4685	0.616 _(30,16) , 0.294		-0.0146 _(0,0501) 0.0586 _(0,0514)
Stroke duration (ms)	Control	118.667±7.186	43.333± 3.783	0.0022 _(36,10) , 0	5.3555 _(1,0000)
	Treatment	98±5.245	43.667± 3.740	0 _(142,5,22) , 0	3.4430 _(1,0000)
	$P_{U(U-stat, df)}$, P_{Perm} Effect Size (P_{Power})	0.0347 _(13,16) , 0.0150	0.7422 _(32,16) , 0.6444		-1.1622 _(0,5885) 0.0316 _(0,0504)
Nose oscillation (BL)	Control	0.200±0.014	n/a	n/a	n/a
	Treatment	0.230±0.007	n/a	n/a	n/a
	$P_{U(U-stat, df)}$, P_{Perm} Effect Size (P_{Power})	0.0831 _(55,16) , 0.0430			0.9105 _(0,4022)
Tail oscillation (BL)	Control	0.353±0.034	0.078±0.011	0.0022 _(36,10) , 0	4.4149 _(0,1000)
	Treatment	0.287±0.016	0.087±0.013	0 _(144,22) , 0	3.9628 _(1,0000)
	$P_{U(U-stat, df)}$, P_{Perm} Effect Size (P_{Power})	0.1025 _(18,16) , 0.0460	0.4371 _(45,16) , 0.1968		-0.8679 _(0,3716) 0.2662 _(0,0792)
Nose elevation (BL)	Control	0.038±0.005	0.003±0.001	0.0022 _(36,10) , 0	2.6018 _(0,9814)
	Treatment	0.0614±0.0076	0.004±0.001	0 _(144,22) , 0	2.4703 _(0,9999)
	$P_{U(U-stat, df)}$, P_{Perm} Effect Size (P_{Power})	0.0529 _(57,16) , 0.0240	0.2908 _(48,16) , 0.1249		1.3210 _(0,6989) 0.2193 _(0,0697)
Fin elevation (FL)	Control	1.052±0.122	0.498±0.068	0.0022 _(36,10) , 0	2.3848 _(0,9599)
	Treatment	0.642±0.067	0.510±0.029	0.0597 _(105,22) , 0.0290	0.8420 _(0,5049)
	$P_{U(U-stat, df)}$, P_{Perm} Effect Size (P_{Power})	0.013 _(10,16) , 0.006	0.8200 _(39,16) , 0.3966		-1.4652 _(0,7855) 0.0797 _(0,0526)
XY fin motion (FL)	Control	2.257±0.223	1.112±0.036	0.0022 _(36,10) , 0	2.9265 _(0,9951)
	Treatment	1.723±0.126	1.142±0.113	0.0023 _(123,22) , 0.0010	1.4003 _(0,9061)
	$P_{U(U-stat, df)}$, P_{Perm} Effect Size (P_{Power})	0.041 _(14,16) , 0.024	1 _(36,16) , 0.4665		-1.0382 _(0,4966) 0.1323 _(0,0571)
Maximum nose velocity (BL/sec)	Control	4.720± 0.394	0.780±0.068	0.0022 _(36,10) , 0	5.7572 _(1,0000)
	Treatment	5.174±0.390	0.804± 0.059	0 _(144,22) , 0	4.5373 _(1,0000)
	$P_{U(U-stat, df)}$, P_{Perm} Effect Size (P_{Power})	0.3845 _(46,16) , 0.1698	0.9636 _(37,16) , 0.4166		0.4119 _{(0,1212)*} 0.1338 _(0,0573)
Maximum tail velocity (BL/sec)	Control	12.564±1.076	1.567±0.221	0.0022 _(36,10) , 0	4.8292 _(1,0000)
	Treatment	11.141±0.850	1.490±0.186	0 _(144,22) , 0	4.3999 _(1,0000)
	$P_{U(U-stat, df)}$, P_{Perm} Effect Size (P_{Power})	0.291 _(24,16) , 0.119	0.8916 _(34,16) , 0.3976		-0.5198 _(0,1647) -0.1345 _(0,0573)
Maximum fin velocity (FL/sec)	Control	3.436±0.434	1.654±0.170	0.0022 _(36,10) , 0	2.2058 _(0,9298)
	Treatment	3.000±0.174	1.677±0.091	0 _(141,22) , 0	2.7453 _(0,1000)
	$P_{U(U-stat, df)}$, P_{Perm} Effect Size (P_{Power})	0.5532 _(29,16) , 0.2448	0.6820 _(41,16) , 0.3107		-0.4610 _(0,1397) 0.0609 _(0,0515)
Fin arc (FL)	Control	3.226± 0.402	1.148±0.043	0.0022 _(36,10) , 0	2.9646 _(0,9958)
	Treatment	2.851±0.172	1.228±0.097	0 _(144,22) , 0	3.5372 _(1,0000)
	$P_{U(U-stat, df)}$, P_{Perm} Effect Size (P_{Power})	0.3845 _(26,16) , 0.1758	0.5532 _(43,16) , 0.2358		-0.4241 _(0,1256) 0.3833 _(0,1114)

* The Kolmogorov–Smirnov goodness-of-fit test showed that all comparisons had at least one non-normal sample. The non-parametric Levene’s test was conducted to check for equal variance; the majority of samples had equal variance.

† All comparisons were made using the Mann–Whitney U-test (P_U) and permutation tests (P_{Perm}).

‡ Path curvature was measured as k , which is 1 divided by the radius of the circle that defines the curve. Therefore, a small k denotes a straight path. Body curvature was calculated as the distance between the nose and the tail tip divided by the fish length; therefore, a smaller value denotes a larger body curvature.

Extended Data Table 2 | Magnitudes of kinematic variables during walking

Variable*	Group	Walk mean \pm s.e.m.
Fin plant duration (ms)	Control	106.785 \pm 20.799
	Treatment	68.129 \pm 5.390
	$P_{U(U\text{-stat, df})}$, P_{Perm} †	0.0415 _(14,16) , 0.0140
	Effect size _(power)	-0.8884 _(0.3862)
Fin slide duration (ms)	Control	54.012 \pm 3.828
	Treatment	38.421 \pm 4.930
	$P_{U(U\text{-stat, df})}$, P_{Perm}	0.032 _(13,16) , 0.0120
	Effect size _(power)	-1.2664 _(0.6623)
Duty factor	Control	0.679 \pm 0.063
	Treatment	0.634 \pm 0.031
	$P_{U(U\text{-stat, df})}$, P_{Perm}	0.2908 _(24,16) , 0.1339
	Effect size _(power)	-0.318 _(0.0820)
Slide factor	Control	0.343 \pm 0.031
	Treatment	0.322 \pm 0.050
	$P_{U(U\text{-stat, df})}$, P_{Perm}	0.1797 _(21,16) , 0.0749
	Effect size _(power)	-0.1858 _(0.0641)
Fin slide distance (mm)	Control	15.807 \pm 1.577
	Treatment	10.617 \pm 1.046
	$P_{U(U\text{-stat, df})}$, P_{Perm}	0.0245 _(12,16) , 0.0060
	Effect size _(power)	-1.3695 _(0.7297)
Fin distance to body short (mm)	Control	36.32 \pm 17.007
	Treatment	9.96 \pm 3.055
	$P_{U(U\text{-stat, df})}$, P_{Perm}	0.0148 _(9.5,16) , 0.0030
	Effect size _(power)	-0.7522 _(0.2932)

* The Kolmogorov–Smirnov goodness-of-fit test showed that all comparisons had at least one non-normal sample. The non-parametric Levene's test was conducted to check for equal variance; the majority of samples had equal variance.

† All comparisons were made using the Mann–Whitney U -test (P_U) and permutation tests (P_{Perm}).

Extended Data Table 3 | Timing of kinematic variables during walking

	Treatment and Control Groups Combined		Treatment Group		Control Group		Comparison between groups	
	μ^*	P_R^\dagger	μ^*	P_R^\dagger	μ^*	P_R^\dagger	$P_{F(F-stat, df1, df2)}, P_{Perm}^\ddagger$	Effect Size [§]
Maximum body curvature	0.41	0.00					0.4612 _(0.570, 1, 16) , 0.4745	0.109
Minimum body curvature	2.26	0.00					0.1524 _(2.258, 1, 16) , 0.1548	-0.407
Left tail amplitude	-2.69	0.00					0.6108 _(0.269, 1, 16) , 0.6284	0.815
Right tail amplitude	0.46	0.00					0.8216 _(0.053, 1, 16) , 0.8132	-0.276
Maximum nose elevation	1.52	0.00					0.3908 _(0.778, 1, 16) , 0.3646	0.120
Maximum fin forward position			0.30	0.00	0.41	0.07	n/a	n/a
Maximum fin backward position			-3.14	0.00	-1.78	0.52	n/a	n/a
Fin plant start	0.37	0.00					0.9237 _(0.010, 1, 16) , 0.9191	-1.620
Fin plant end			-2.75	0.00	-1.15	0.91	n/a	n/a
Fin slide start			1.40	0.00	0.87	0.00	0.0221 _(6.426, 1, 16) , 0.0170	-1.517
Fin slide end			2.57	0.00	-3.08	0.08	n/a	n/a
Minimum fin distance from body midline			2.39	0.00	2.16	0.55	n/a	n/a

*Time at which the variable occurs, in radians. All variables had an equal variation and did not differ from a von Mises distribution (Kuiper test, $P > 0.05$). P_R values for each group were calculated using Rayleigh's test for circular uniformity.

† $P_R < 0.05$ represents variables with significant directionality.

‡ Comparisons of angles with significant directionality between groups calculated using the Watson–Williams multiple comparison test (P_F) and permutation tests (P_{Perm}).

§ Power is not included here, as a clear power analysis for circular statistics is lacking in the literature.

Extended Data Table 4 | Timing of kinematic variables during swimming

Variable	Treatment and Control Groups Combined		Treatment Group		Control Group		Comparison between groups	
	μ^*	P_R^\dagger	μ^*	P_R^\dagger	μ^*	P_R^\dagger	$P_{F/(F-stat, df1, df2)}, P_{Perm}^\ddagger$	Effect Size [§]
Maximum body curvature	1.54	0.00					0.8863 _(0.0211, 1, 16) , 0.8611	0.470
Minimum body curvature	1.73	0.00					0.7840 _(0.0777, 1, 16) , 0.7622	-0.078
Left tail amplitude			-0.21	0.28	-2.93	0.00	n/a	n/a
Right tail amplitude			2.75	0.02	2.16	0.69	n/a	n/a
Max nose elevation	1.61	0.00					0.3411 _(0.9668, 1, 16) , 0.3596	0.582
Fin up	0.28	0.00					0.4227 _(0.6771, 1, 16) , 0.4146	0.580
Fin down	2.83	0.00					0.4262 _(0.6666, 1, 16) , 0.4306	0.447

* Time at which the variable occurs, in radians. All variables had an equal variation and did not differ from a von Mises distribution (Kuiper test, $P > 0.05$). P_R values for each group were calculated using Rayleigh's test for circular uniformity.

$\dagger P_R < 0.05$ represents variables with significant directionality.

\ddagger Comparisons of angles with significant directionality between groups calculated using the Watson–Williams multiple comparison test (P_F) and permutation tests (P_{Perm}).

\S Power is not included here, as a clear power analysis for circular statistics is lacking in the literature.

Extended Data Table 5 | Analysis of variance (ANOVA) comparison of size regression models

	$P_{F(F\text{-stat}, df_{num}, df_{den})}$, P_{Perm}	% variance accounted by size	
Clavicle	0.3783 _(1,133,4,15) , 0.388	9.150	
Cleithrum	0.3422 _(1,224,4,15) , 0.351	34.316	
Supracleithrum	0.0143 _(4,455,4,15) , 0.014	21.526*	33.437*

* Computed separately for control (left) and treatment (right) groups.

Extended Data Table 6 | Fish size

	Treatment \pm s.e.m.	Control \pm s.e.m.	P-value*
Fish length before (mm)	69.01 \pm 0.007	77.29 \pm 0.0100	<0.0001
Fish weight before (g)	1.72 \pm 0.0004	2.28 \pm 0.0011	<0.0001
Fish length after (mm)	77.41 \pm .0116	102.31 \pm 0.0265	<0.0001
Fish weight after (g)	2.44 \pm 0.0015	6.11 \pm 0.0066	<0.0001

* Calculated with a Kolmogorov–Smirnov test between each distribution.